

Square versus Roll Pattern at Convective Threshold

P. Le Gal, A. Pocheau, and V. Croquette

Service de Physique du Solide et de Résonance Magnétique, Centre d'Etudes Nucléaires de Saclay, F-91191 Gif-sur-Yvette, France
(Received 5 March 1985)

We present observations and measurements of convection between two moderately conducting plates. A stationary square pattern is observed just at the convective threshold. But at high Rayleigh number the preferred convective pattern becomes the usual roll structure. The transition from squares to rolls involves an unexpected Hopf bifurcation.

PACS numbers: 47.25.Qv, 47.20.+m

The study presented here was motivated by the observation of a squarelike cellular convective pattern at convection threshold in a Rayleigh-Bénard experiment, with horizontal sapphire boundaries which conduct heat well.¹ This structure disappeared as soon as we increased the Rayleigh number N_R and left a classical roll structure. As some theoretical studies predict square patterns at threshold resulting from poorly heat-conducting boundaries, we have hypothesized that the large but finite thermal conductivity of sapphire is at the origin of our square pattern.

Some experiments have already been performed with poor thermal conductors but they have not investigated the convective pattern just at threshold.²⁻⁴ We therefore replaced our sapphire plates by glass slabs of similar dimensions but having a lower heat conductivity. We then observed and measured clear square-pattern convection near threshold, stable in a domain of Rayleigh number larger than in the sapphire case, so that we were able to study the evolution of the pattern from squares to rolls. We were surprised to find that it occurs through a Hopf bifurcation leading to oscillation of the entire structure.

This square pattern has nothing to do with high-Rayleigh-number bimodal convection,² which involves two very different sets of rolls. The observation of such a time-dependent behavior so close to the threshold is, as far as we know, completely new and should make it amenable to analysis by a perturbation expansion.

The cell consists of a Plexiglas annulus placed between two glass discs. The height of this cylindrical cell is 1.975 mm and its aspect ratio (radius/height: R/d) is 20. The glass plates are 6 mm thick.

We used a 5-centistoke silicone oil whose Prandtl number N_P (ν/κ) equals 70. The thermal conductivity ratio β between glass and oil is 7. This setup is placed between two other glass plates, which permits thermal regulation by water circulation. This apparatus, completely transparent, allows optical measurements.

Overall qualitative information is derived from shadowgraph and Schlieren pictures or movies. Local quantitative measurements are obtained by a recording

of the deflection of a laser beam induced by the index gradient inherent to convective motions. A photodiode measures the two components of the index gradient integrated over the height of the cell. A microcomputer monitors stepper motors and scans the convective pattern on a square lattice of 16×16 points extending typically over four convective wavelengths. The amplitudes of the convective modes are obtained by performing a two-dimensional fast Fourier transformation (2D FFT).⁵

In the experiment, we measure the temperature difference between the water circulation at the top and at the bottom which, because of the heat conductivity of the boundaries, differs from that applied to the oil layer. We then evaluate the reduced Rayleigh number $\epsilon = (N_R - N_{Rc})/N_{Rc}$ taking into account the convective heat flux.⁶

The different features that we present here have been obtained by use of "perfect" patterns, that is, convective structures without any structural defect. Such structures were initiated by induction of a parallel roll structure at high Rayleigh number by the method of Chen and Whitehead.⁷

After the induction, if we lower the reduced Rayleigh number ϵ below 0.024, we observe a stationary square pattern. This means that a second set of rolls has appeared perpendicular to the first set with the same wave number and with an amplitude which is quite close, as seen in Fig. 1(a). This square pattern also appears when we increase the Rayleigh number above the convective threshold without proceeding through any induction. But in this case the square pattern contains several structural defects.

The bifurcation between the conductive and the convective state seems imperfect, as we may see in Fig. 2. The Plexiglas sidewall, whose conductivity is twice that of the oil, may produce horizontal thermal gradients at the sidewall. But in this case the convection should appear first at the sidewall. On the contrary, we observe that the convective pattern appears first in the center of the convective cell.

When we increase ϵ above 0.024, a Hopf bifurcation takes place and the amplitudes A and B , measured with the 2D-FFT technique in the center of the cell, exhibit

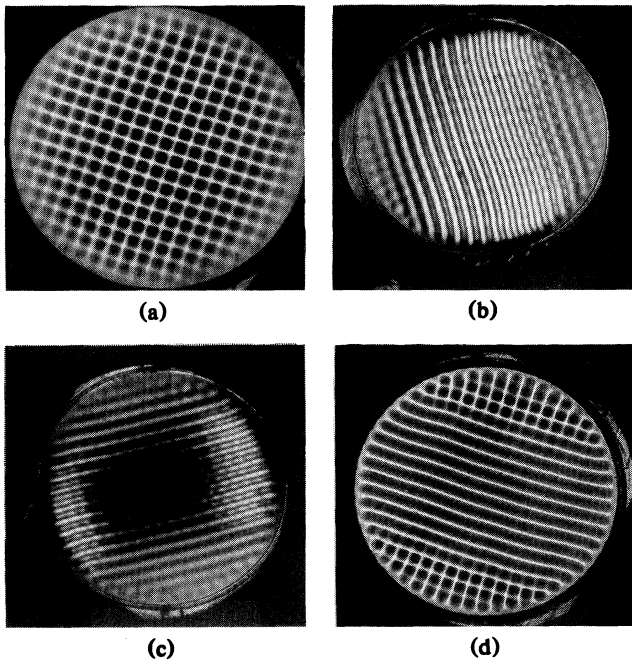


FIG. 1. (a) Focalization picture of a stationary square pattern, $\epsilon = 0.020$. Notice that this structure is accommodated quite well in the cylindrical cell. The white lines represent cold streams and the dark lines hot streams. This picture has the periodicity of the convective structure. (b),(c) Strioscopic pictures of the oscillating square structure, $\epsilon = 0.047$. Using this technique, we are able to isolate a single system of rolls. Each white line corresponds to the center of a roll so that the picture presents a periodicity twice that of the convective pattern. These two pictures correspond to the same structure: (b) shows the dominant roll set and (c) the perpendicular roll set. (d) Focalization picture of the stationary roll pattern, $\epsilon = 0.2$: The dominant roll set has invaded nearly the entire cell, leaving only two small grain boundaries.

oscillating behavior in phase opposition with time. At $\epsilon_h = 0.024$ the oscillation is barely visible and quite sinusoidal. Its amplitude increases with ϵ and finally the oscillation exhibits a relaxation behavior, as can be seen in Fig. 3. A movie of this phenomenon shows that the two perpendicular sets of rolls alternately invade nearly the entire cell. The symmetry (over one period) between the two sets is conserved when $\epsilon_h < \epsilon < 0.057$, as may be seen in Figs. 3(a) and 3(b), but it breaks down when $\epsilon > 0.057$, and leaves one set of rolls dominant. This last point clearly appears on our amplitude recordings, plotted in Fig. 3(c), where A^2 is greater than B^2 while both signals still show oscillating behavior. The set of rolls whose amplitude is greater when $\epsilon = 0.057$ is reached remains as the dominant one. From the movie, it appears that the dominant set extends from one side of the cell to the opposite side cutting the second set into two parts [see Figs.

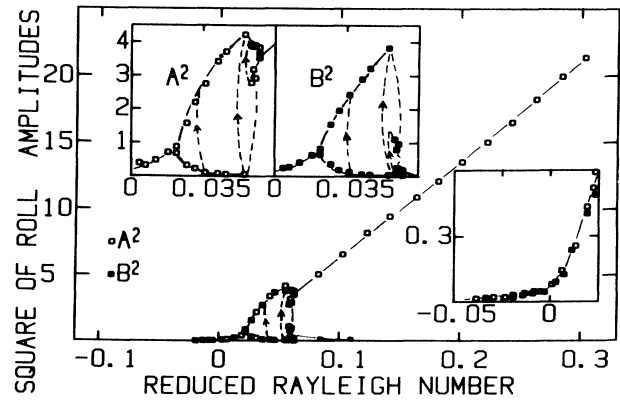


FIG. 2. Square of the roll amplitudes A^2 and B^2 (in arbitrary units), obtained by our performing of a 2D FFT of the pattern center, vs the reduced Rayleigh number ϵ . Notice that the stationary square pattern is limited to a very small domain in ϵ , $\epsilon < 0.024$, and that the oscillating region is confined in the range $0.024 < \epsilon < 0.057$. In the lower right corner we have redrawn an enlarged portion of this curve in the vicinity of the threshold. In the upper left corner we have drawn separately the behavior of both roll amplitudes in the oscillatory regime. In this picture it is the set of rolls with the amplitude A which becomes dominant when we increase ϵ .

1(b) and 1(c)]. These two parts, which are next to the sidewalls, periodically extend—trying, one might say, to join at the center—but do not succeed and retreat towards the sidewall. As we slightly increase ϵ these two parts become confined to the sidewall, leaving most of the cell to the dominant roll set. This description is also valid in the symmetric oscillatory phase, except that the two parts succeed in joining, and the

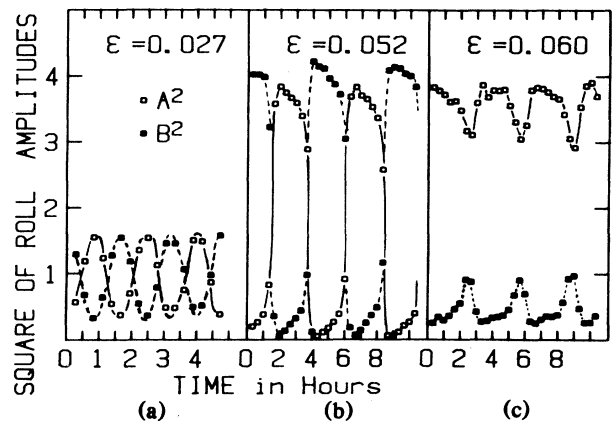


FIG. 3. Time recordings of the square of the roll amplitudes (in arbitrary units) in the oscillatory regime. The amplitudes have been obtained with the 2D-FFT technique. (a) Sinusoidal oscillation. (b) Relaxational oscillation. (c) The symmetry between the two roll sets is now broken, but oscillatory behavior is still present.

roles of the two sets are inverted.

In the asymmetric oscillatory regime, a slight increase in ϵ causes the dominant set of rolls to invade nearly the entire cell, confining the two oscillating grain boundaries very near the sidewalls [see Fig. 1(d)]. The oscillation then becomes barely visible. At the center of the cell the convective pattern has the appearance of the classical stationary roll pattern.

A square pattern has been predicted in the case of poorly conducting horizontal boundaries in various studies,^{8,9} which rely on the assumption that β tends to 0. This is far from our situation, especially since those studies use the property that the wave number K_c tends to 0 with β , while in our case $K_c = 3.00 \pm 0.05$, close to the value 3.117 obtained when β tends to infinity. However, Jenkins and Proctor¹⁰ investigated the full domain of β and determined the regions in the (β, N_p) plane where squares and rolls should be observed. With the N_p we used, they conclude that squares should be observed when $\beta < 1$ and rolls when $\beta > 1$, but this is not the case. This contradiction is even stronger when we consider the square pattern observed with the sapphire boundaries ($\beta = 250$), in a similar apparatus. In fact, when β equals infinity, the square pattern has been found to be only weakly unstable and is stabilized by a temperature dependence of a convective parameter.¹¹

Following Newell and Whitehead¹² we introduce two coupled amplitude equations describing the square pattern:

$$dA/dt = \epsilon A - EA^2A^* - FABB^*, \quad (1a)$$

$$dB/dt = \epsilon B - EB^2B^* - FBAA^*, \quad (1b)$$

where A and B are the amplitudes of each set of rolls, and E and F parameters of nonlinearity. If $E > F$ the stationary state corresponds to the case of spatially homogeneous equal amplitudes $A^2 = B^2 = \epsilon/(E + F)$ and thus to a square pattern. Experimentally, we found this type of Landau evolution (see Fig. 2). On the contrary, if $F > E$ the stationary solution of Eqs. (1) is a roll pattern with an amplitude $A^2 = \epsilon/E$. The transition occurs when $E = F$ and in its vicinity one may notice that the ratio between the two slopes $E/(E + F) = \frac{1}{2}$. (When N_p and β tend to infinity it equals $1/2.2273$.¹³)

The oscillating behavior may be seen as a transition from a square pattern to a roll pattern. As far as we know this kind of transition has not yet been studied. The dynamical behavior is especially interesting since it occurs very near the convective threshold where perturbation analysis should apply. However, the amplitude equations (1) cannot describe this transition since, being derived from a potential, they forbid any oscillatory behavior. We have not yet arrived at any convincing interpretation of this oscillation. As in Nicolis and Prigogine,¹⁴ we have considered the non-

variational Volterra-type amplitude equations¹⁵ for which oscillatory behavior is possible. However, this model, which is spatially homogeneous, requires that the two sets of rolls be so strongly different that this cannot correspond to our situation. It appears from the film that the spatio-temporal features are related to the geometry of the cell, since the period of oscillation is determined by the transit time of the grain boundaries through the cell. From the 2D-FFT measurements in the center of the cell, the oscillation occurs with a Hopf bifurcation at $\epsilon_h = 0.024$ (see Fig. 1), its amplitude increases as $(\epsilon - \epsilon_h)^{1/2}$, and its period grows from 4600 s at ϵ_h to 16 800 s when $\epsilon = 0.0057$. This long time can only be compared to the horizontal thermal diffusion time $R^2/Dt = 22 500$ s, and we plan to perform further experiments with different cell geometries in order to test this relation.

As we see in Fig. 2, the stationary roll amplitude obeys a Landau-type law but its extrapolated threshold differs from that of squares: $\epsilon_r = 0.012$. However, the ratio between the slopes of A^2 vs ϵ in stationary squares and in rolls equals $\frac{1}{2}$ within a few percent, as predicted by Eqs. (1) near the square-to-roll pattern transition.

In this experiment we have observed and measured a square convective pattern which is stable near the convective threshold and destabilizes in favor of the usual roll pattern when we increase ϵ . Koschmieder⁴ has also observed a square pattern near threshold but it was unstable and he argued that this pattern was generated by the square container he used. Obviously, this argument cannot hold with our cylindrical cell. However, Koschmieder also used a glass plate at the top and this confirms the qualitative idea that the square pattern is related to the conductivities of the horizontal boundaries as inferred by theoretical studies. Nevertheless, our results are in quantitative disagreement with these predictions.

We therefore propose the following assertion: As long as the heat conductivity of the horizontal boundaries is finite, convection at high Prandtl number appears at threshold with a square pattern, but becomes a roll pattern at higher Rayleigh number, the domain of ϵ where squares exist becoming smaller as β is increased. To be specific, when $\beta = 7$ the domain extends up to $\epsilon = 0.057$, while with $\beta = 250$ it is just visible and we estimate its extension to be 0.003. It would be interesting to check our assertion and to determine if the finite conductivity is the only origin of the square pattern, since it seems that strong dependence of the viscosity on the temperature might also induce a square pattern.¹⁶ Note that this pattern selection is reminiscent of that which occurs with hexagons and rolls in non-Boussinesq Rayleigh-Bénard convection¹⁷ (except for the dynamical behavior).

The nature of the convective pattern at threshold is

the first step in the understanding of convection. Here we have observed a square pattern whose three-dimensionality could lead to unexpected behavior such as our oscillatory regime. The very existence of such a regime raises the problem of the nonvariational character of convection in finite-size containers near threshold.

We are grateful to M. Dubois, P. Bergé, P. Manneville, L. Tuckerman, and Y. Pomeau for stimulating discussions, and to C. Poitou, M. Labouise, and B. Ozenda for their technical assistance.

¹V. Croquette, M. Mory, and F. Schosseller, *J. Phys. (Paris)* **44**, 293 (1983).

²J. A. Whitehead, Jr. and B. Parsons, *Geophys. Astrophys. Fluid Dyn.* **9**, 201–217 (1978).

³M. Dubois, Thesis, Université de Paris VI, 1976 (unpublished); P. Bergé and M. Dubois, *Phys. Rev. Lett.* **32**, 1041 (1974).

⁴E. L. Koschmieder, *Beitr. Phys. Atmos.* **39**, 1–11 (1966).

⁵We may use such a small number of points per wavelength, since we have checked with scans over 32×32 points that the signals are very sinusoidal. The FFT was performed with a cosine window weighting. Peak amplitude is obtained by summation of nine adjacent channels centered on it. We estimate the error on the amplitude to be 0.1 in the units of Figs. 2 and 3. A similar technique is described in J. P. Gollub and A. R. McCarriar, *Phys. Rev. A* **26**, 3470–3476 (1982).

⁶We have evaluated the heat flux using the following Nusselt law: $N_N - 1 = [\epsilon / (1 + \epsilon)](0.69942 - 0.00472N_p^{-1})$

found in A. Schlüter, D. Lortz, and F. Busse, *J. Fluid Mech.* **23**, 1296 (1965). In our case $\epsilon = 0.6024(\delta T - \delta T_c) / \delta T_c$, where δT is the measured temperature difference.

⁷M. M. Chen and J. A. Whitehead, Jr., *J. Fluid Mech.* **31**, 1 (1968).

⁸F. H. Busse and N. Riahi, *J. Fluid Mech.* **96**, 243–256 (1980); N. Riahi, *Z. Angew. Math. Phys.* **31**, 261 (1980).

⁹M. R. E. Proctor, *J. Fluid Mech.* **113**, 469 (1981).

¹⁰D. R. Jenkins and M. R. E. Proctor, *J. Fluid Mech.* **139**, 461–471 (1984).

¹¹H. Frick, F. H. Busse, and R. M. Clever, *J. Fluid Mech.* **127**, 141–153 (1983), show that squares are weakly unstable when β equals infinity. In F. H. Busse and H. Frick, *J. Fluid Mech.* **150**, 451–463 (1985), it is found that squares are stabilized by a strong temperature-dependent viscosity. However, as the dependence is weak in our case ($r = 1.12$) this result does not predict stability of our square pattern. As our two experiments ($\beta = 250$ and $\beta = 7$) were conducted under otherwise identical conditions, in particular with identical r , the difference we observed in the stability range of the square pattern can only be attributed to β .

¹²A. C. Newell and J. A. Whitehead, Jr., *J. Fluid Mech.* **38**, 279 (1969).

¹³P. Manneville and Y. Pomeau, *Philos. Mag. A* **48**, 607–621 (1983).

¹⁴G. Nicolis and I. Prigogine, *Self-Organization in Nonequilibrium Systems* (Wiley, New York, 1977).

¹⁵J. Guckenheimer and P. Holmes, *Nonlinear Oscillations, Dynamical Systems, and Bifurcations of Vector Fields* (Springer-Verlag, New York, 1983), p. 405.

¹⁶D. S. Oliver and J. R. Booker, *Geophys. Astrophys. Fluid Dyn.* **27**, 73–85 (1983).

¹⁷M. Dubois, P. Bergé, and J. Wesfreid, *J. Phys. (Paris)* **39**, 1253–1257 (1978).

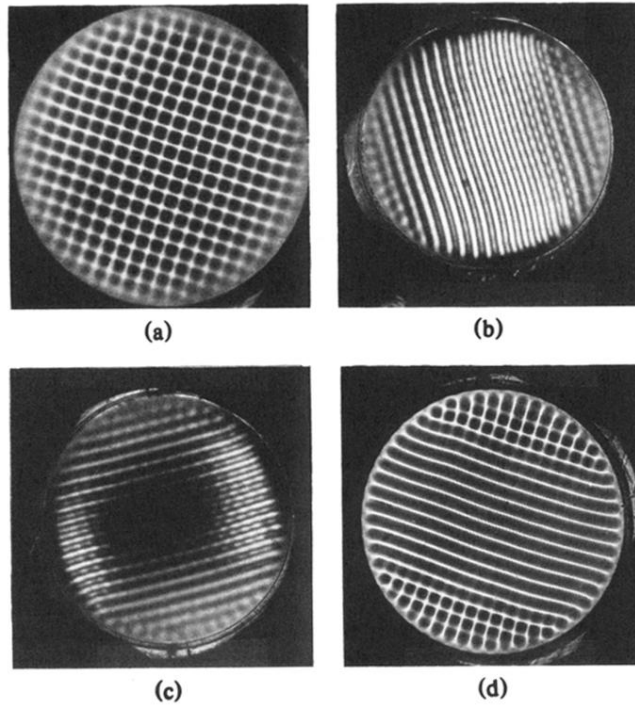


FIG. 1. (a) Focalization picture of a stationary square pattern, $\epsilon = 0.020$. Notice that this structure is accommodated quite well in the cylindrical cell. The white lines represent cold streams and the dark lines hot streams. This picture has the periodicity of the convective structure. (b),(c) Strioscopic pictures of the oscillating square structure, $\epsilon = 0.047$. Using this technique, we are able to isolate a single system of rolls. Each white line corresponds to the center of a roll so that the picture presents a periodicity twice that of the convective pattern. These two pictures correspond to the same structure: (b) shows the dominant roll set and (c) the perpendicular roll set. (d) Focalization picture of the stationary roll pattern, $\epsilon = 0.2$: The dominant roll set has invaded nearly the entire cell, leaving only two small grain boundaries.